J. Chem. Thermodynamics 91 (2015) 17–29

Contents lists available at ScienceDirect

J. Chem. Thermodynamics

journal homepage: www.elsevier.com/locate/jct

Density measurements on binary mixtures (nitrogen + carbon dioxide and argon + carbon dioxide) at temperatures from (298.15 to 423.15) K with pressures from (11 to 31) MPa using a single-sinker densimeter

Xiaoxian Yang [a], Markus Richter [b], Zhe Wang [a,*], Zheng Li [a]

[a] State Key Laboratory of Power Systems, Department of Thermal Engineering, Tsinghua University, Beijing 100084, PR China
[b] Lehrstuhl für Thermodynamik, Ruhr-Universität Bochum, D-44780 Bochum, Germany

ARTICLE INFO

Article history:
Received 14 April 2015
Received in revised form 14 July 2015
Accepted 15 July 2015
Available online 22 July 2015

Keywords:
Single-sinker densimeter
Fluid density
Binary mixture
Carbon dioxide
Nitrogen
Argon

ABSTRACT

A single-sinker densimeter was built to specifically investigate the (p,ρ,T,x) behavior of fluid mixtures relevant for carbon capture and storage (CCS). Due to the use of a magnetic-suspension coupling, the densimeter enables measurements over the temperature range from (273.15 to 423.15) K with pressures up to 35 MPa. A comprehensive analysis of the experimental uncertainties was undertaken. The expanded uncertainties ($k = 2$) are 35 mK for temperature, 3.39 kPa for pressure, and 0.033% for density determination. The apparatus was used for measurements on the binary systems (nitrogen + carbon dioxide) and (argon + carbon dioxide). The compositions for both systems were (0.05 and 0.01) mole fraction carbon dioxide. Density measurements were carried out at temperatures from (298.15 to 423.15) K with pressures from (11 to 31) MPa. The relative combined expanded uncertainty ($k = 2$) in density was 0.15% for the (nitrogen + carbon dioxide) mixtures and 0.12% for the (argon + carbon dioxide) mixtures. A major contribution to this uncertainty emerged from the uncertainty in the gas mixture composition. The new experimental data were compared to the GERG-2008 equation of state (EOS) for natural-gas mixtures as implemented in the NIST REFPROP database and to the EOS-CG, another new Helmholtz energy model for CCS mixtures as implemented in the TREND software package of Ruhr-University Bochum. Relative deviations were mostly within 0.5%. The agreement of the new density values with the only available literature data closest to the composition range under study was better than 0.1%.

1. Introduction

The single-sinker densimeter (SSD) is one of the state-of-the-art instruments to accurately measure the density of fluid substances over large temperature and pressure ranges. The method is based on the Archimedes buoyancy principle and can be used as an absolute technique without the need for calibration fluids. The commonly used reference equations of state (EOS), *e.g.*, for nitrogen [1], argon [2], carbon dioxide [3], ethane [4], ethylene [5], propane [6], and sulfur hexafluoride [7] were all modeled with the help of data measured with SSDs. Moreover, with the increasing demand for knowledge of volumetric properties of fluid mixtures, more measurements [8–11] were carried out utilizing different SSDs. However, in this context only accurate density data of binary mixtures serve to further improve the performance of multi-parameter EOS for mixtures, especially those based on the GERG EOS (GERG-2004 of Kunz *et al.* [12] and GERG-2008 of Kunz and Wagner [13]). All reference EOS play important roles in various engineering applications, such as refrigeration engineering [14], oil and gas engineering [15], and in the field of carbon capture and storage (CCS) [16].

The SSD was developed by Brachthäuser *et al.* [17,18] in the early 1990s. It simplifies the complex design of the two-sinker densimeter [19] when only measurements of medium and high densities are the goal. An overview of this general type of instrument incorporating a magnetic suspension coupling was published by Wagner and Kleinrahm [20] as well as in chapter 2 of [21] by McLinden. Different versions of the SSD were built by research groups all over the globe [22–27]. A selection of different SSDs, including measuring range, system uncertainty, and measured fluids, is listed in table 1. Each SSD has its unique features, either of extreme low uncertainty, *i.e.*, a few parts per million in Kuramoto's group [22], or of a large pressure range, *i.e.*, up to

* Corresponding author. Tel.: +86 13811902238.
E-mail address: zhewang@tsinghua.edu.cn (Z. Wang).

http://dx.doi.org/10.1016/j.jct.2015.07.014
0021-9614/

TABLE 1
Measuring range, system uncertainty and measured fluids of selected single-sinker densimeters.

	Range and Uncertainty ($k = 2$)			
Group	Temperature	Pressure	Density	Measured fluids
Hall	(193.15 to 523.15) K [9]	Up to 200 MPa [9]	0 to 2000 kg/m^3 [9]	CO_2 [29], C_2H_6 [30], N_2 [28], CH_4 [31], natural gases [8,9,15,32,33]
	5.0 mK [9]	0.01% of (40 or 200) MPa [28]	0.1% [9]	
Chamorro	(250 to 400) K [25]	Up to 20 MPa [25]	0 to 2000 kg/m^3 [25]	CH_4-N_2 [34], CO_2-N_2 [10,35], CH_4-CO_2 [36], $CO-N_2$ [37]
	3.9 mK [25]	(0.007 to 0.015)% of 20 MPa [25]	(0.020 to 0.155)% [25]	
Kuramoto	(293.15 to 473.15) K [22]	Designed up to 20 MPa [22]	n/a	*iso*-Octane, *n*-nonane, *n*-tridecane, water, 2,4-dichlorotoluene, 3,4-dichlorotoluene, bromobenzene [22]
	3.0 mK [22]	n/a	(6.7 to 11.7) ppm [22]	
Wagner	(235 to 520) K [38]	Up to 30 MPa [39]	(2 to 2000) kg/m^3 [39]	Cyclohexane, toluene, and ethanol [39], *n*-heptane, *n*-nonane, 2,4-dichlorotoluene, and bromobenzene [40], Ethylene, ethane, and sulfur hexafluoride [38], Ar and N_2 [41], CH_4 and CO_2 [42]
	8.0 mK [39]	0.006% or 50 Pa [39]	0.015% [39]	
Span I	(90 to 290) K	(0.05 to 12) MPa	10 to 1000 kg/m^3	Designed for measurements on cryogenic liquid mixtures [26,27], currently in use for density measurements of LNG mixtures
	15.0 mK	0.01%	0.01% (for liquids)	
Span II	(235 to 475) K	Up to 20 MPa	2 to 2000 kg/m^3	Currently in use for gas phase density measurements of CCS mixtures [43]
	15.0 mK	0.01%	0.02%	
Our group	(273.15 to 423.15) K 35 mK	Up to 35 MPa 3.39 kPa	2 to 2000 kg/m^3 0.033%	CO_2-N_2, CO_2-Ar

200 MPa in Hall's group [9], or for the use at cryogenic temperatures as at Ruhr-University Bochum [26,27]. Recently a new SSD (type: FluiDENS, Rubotherm, Germany) was installed in our laboratory at Tsinghua University. The apparatus was built to specifically investigate the (p,ρ,T,x) behavior of fluid mixtures relevant for CCS. To enable the investigation of supercritical states, as well as of corrosive substances, the densimeter was designed for measurements over the temperature range from (273.15 to 423.15) K with pressures up to 35 MPa.

CCS is considered to be one of the most important strategies in reducing global carbon emissions [44]. The fluids involved in the pipeline transportation in CCS are mainly carbon dioxide, argon, nitrogen, oxygen, water, sulfur oxide, nitric oxide, and other trace substances [16]. The exact compositions and quantities of the impurities vary with different carbon dioxide sources and different capture and purification processes [16,44,45]. The density of carbon dioxide mixtures is a fundamental parameter in the process design for CCS. However, to the best of our knowledge, the density data situation is poor and the available data are mostly of lacking accuracy. In the present project we focused on the binary mixtures (nitrogen + carbon dioxide) and (argon + carbon dioxide). The available experimental data concerning these binaries are summarized in table 2. No data are available for compositions lower than 0.10 mol fraction carbon dioxide for the binary mixtures under study. To fill this data gap, comprehensive density measurements at temperatures from (298.15 to 423.15) K with pressures from (11 to 31) MPa were carried out on the two binary systems both with compositions (0.05 and 0.01) mole fraction carbon dioxide utilizing the new SSD. Although mixtures with a composition of only (0.01 to 0.05) mole fraction carbon dioxide seem to differ just slightly from the pure major component, experimental densities will reveal helpful information in terms of performance testing (and maybe for the improvement) of multi-parameter EOS, as will be discussed in Section 4.3.

2. Experimental

2.1. Apparatus description

The density measurement system is schematically illustrated in figure 1. It was divided into four sections: gas source, gas pre-treatment, density measurement, and exhaust-gas treatment. The gas source section provided the gas sample under study as well as compressed air to operate the booster pump. In the gas pre-treatment section, the gas was heated by the preheater to a supercritical state. This was required to avoid condensation of gas during compression. Afterwards, the gas was compressed to the designated pressure (maximum to 35 MPa) by means of a booster pump and then stored in a high-pressure (HP) cylinder. The HP cylinder provided the gas sample to the SSD via a thermostated gas-dosing system, which controlled the pressure inside the measuring cell. The pressure line from the outlet of the preheater to the inlet of the gas-dosing system was insulated; especially the HP cylinder was temperature controlled to keep the gas sample in a supercritical state and to increase the pressure of fluid when necessary. A vacuum pump was connected to the HP cylinder to make sure the original sample was completely removed when changing to another fluid. The density measurement section was placed in a protection room where the temperature was kept stable between (293.15 and 298.15) K. The densimeter itself was also connected to a vacuum pump for evacuation of the measuring cell. The exhaust-gas treatment section, which involved using a supersaturated sodium bicarbonate solution to absorb sulfur dioxide, was only operated if required.

A schematic diagram of the SSD is shown in figure 2. It basically consisted of a high-pressure measuring cell, which was installed inside a vacuum-insulated two-stage thermostat, a magnetic-suspension coupling incorporated in the measuring cell, and an analytical balance at the top of the apparatus. Both

TABLE 2
Review of volumetric measurements on CO_2–N_2 and CO_2–Ar.

T/K	p/MPa	x/mole fraction of CO_2	Uncertainty[a] T; p; ρ; (coverage factor)	Author	Year
			$xCO_2 + (1-x)Ar$		
323.15	5.0 to 101.3	0.12 to 0.83	n/a; n/a; n/a; (n/a)	Abraham and Bennett [46]	1960
288.15	2.40 to 14.34	0.70 to 0.94	0.01 K; 0.1 MPa; n/a; (n/a)	Sarashina *et al.* [47]	1971
373.15 to 573.15	0.3 to 59.3	0.18 to 0.80	n/a; n/a; n/a; (n/a)	Schönmann [48]	1971
313.15 to 353.15	5.8 to 58.8	0.20 to 0.71	n/a; n/a; n/a; (n/a)	Kosov and Brovanov [49]	1975
313.15	0.3 to 20.9	0.35 to 0.81	n/a; n/a; n/a; (n/a)	Altunin and Koposhilov [50]	1976
303.15 to 373.15	0.2 to 24.7	0.35 to 0.81	n/a; n/a; n/a; (n/a)	Altunin and Koposhilov [51]	1977
303.15 to 383.15	1.0 to 20.0	0.8306, 0.9692	0.05 K; 0.03%; 0.2 kg/m^3; (n/a)	Mantovani *et al.* [52]	2012
			$xCO_2 + (1-x)N_2$		
273.15 to 473.15	5.0 to 50.6	0.24 to 0.47	n/a; n/a; 0.5%; (n/a)	Kritschewsky and Markov [53]	1940
298.15	0.0 to 0.1	0.48	0.01 K; n/a; 0.002%; (n/a)	Edwards and Roseveare [54]	1942
298.15 to 398.15	3.0 to 50.0	0.2513, 0.5048	n/a; n/a; 0.05%; (n/a)	Haney and Bliss [55]	1944
303.15	0.0 to 0.1	0.49 to 0.50	n/a; n/a; n/a; (n/a)	Gorski and Miller [56]	1953
253.15 to 288.15	2.4 to 14.5	0.46 to 0.94	0.01 K; 0.1 MPa; n/a; (n/a)	Arai *et al.* [57]	1971
323.15 to 343.15	0.3 to 20.4	0.21 to 0.76	n/a; n/a; n/a; (n/a)	Altunin and Chin [58]	1972
313.15 to 353.15	5.9 to 58.8	0.23 to 0.67	n/a; n/a; n/a; (n/a)	Kosov and Brovanov [49]	1975
273.15 to 473.15	0.3 to 9.9	0.18 to 0.98	n/a; n/a; n/a; (n/a)	Rivkin [59]	1975
243.15 to 333.15	2.7 to 19.6	0.90 to 0.95	0.02 K; 0.01 MPa; n/a; (n/a)	Kaminishi [60]	1978
250 to 329	2.2 to 33.0	0.98	0.03 K; 0.01%; 0.02%; (n/a)	Ely *et al.* [61]	1987
323.15, 348.15	49.0 to 273.7	0.25, 0.5, 0.74	0.1 K; 0.25 MPa; (0.5 to 1)%; (n/a)	Hacura *et al.* [62]	1988
300, 320	0.1 to 10.6	0.10 to 0.90	0.005 K; (0.005 to 0.015)%; n/a; (n/a)	Brugge *et al.* [63]	1989
303.15 to 333.15	0.75 to 5.99	0.9998	0.01 K; 0.1%; n/a; (n/a)	McElroy *et al.* [64]	1989
205 to 320	0.1 to 48.4	0.44696	0.01 K; (0.005 to 0.015)% p; n/a; (n/a)	Esper *et al.* [65]	1989
250 to 329	Up to 33.0	0.982	0.008 K; 0.01%; (0.1 to 0.15)%; (n/a)	Ely *et al.* [66]	1989
208 to 400	0.0 to 48.4	0.44	0.01 K; 0.1%; 0.1%; (n/a)	Bailey *et al.* [67]	1989
293.2	0.6 to 5.1	0.27 to 0.70	n/a; 0.01%; n/a; (n/a)	Jiang *et al.* [68]	1990
274 to 349	0.2 to 26.1	0.10 to 0.31	n/a; n/a; n/a; (n/a)	Jaeschke and Humphreys [69]	1991
473.15	100.0	0.10 to 0.90	0.01 K; 0.01 MPa; n/a; (n/a)	Seitz *et al.* [70]	1994
205 to 300	1.1 to 77.5	0.3991, 0.4459, 0.5037	0.01 K; 0.01 MPa; 0.1%; (n/a)	Duarte–Garza *et al.* [71]	1995
225 to 450	0.2 to 69.1	0.10 to 0.90	0.01 K; 0.01 MPa; 0.1%; (n/a)	Duarte–Garza *et al.* [72]	1995
673.15	19.9 to 99.9	0.1 to 0.9	0.05 K; 0.02 MPa; 1 kg/m^3; (n/a)	Seitz and Blencoe [73]	1996
323.15 to 573.15	9.9 to 99.9	0.1 to 0.9	0.05 K; 0.02 MPa; 1 kg/m^3; (n/a)	Seitz *et al.* [74]	1996
225 to 450	Up to 69.1	0.10 to 0.90	0.005 K; 0.006 MPa; 0.1%; (k = 2)	Brugge *et al.* [75]	1997
250 to 400	Up to 19.9	0.1, 0.15	0.0039 K; 0.015%; (0.02 to 0.15)%; (n/a)	Mondéjar *et al.* [35]	2011
303.15 to 383.15	1.0 to 20.0	0.9021, 0.9585	0.05 K; ±0.03%; 0.2 kg/m^3; (n/a)	Mantovani *et al.* [52]	2012
250 to 400	Up to 19.9	0.20, 0.50	0.0039 K; 0.015%; (0.02 to 0.15)%; (k = 2)	Mondéjar *et al.* [10]	2012

[a] The uncertainties listed, are just for information purposes and especially those estimated before 1990 are from a current point of view possibly not reliable because (i) the confidence probability was not provided in the original paper; (ii) there was no general standard to declare the measurement uncertainty at that time; or (iii) no complete analysis on the measurement uncertainty was done for these apparatuses. The uncertainty guidance we followed is GUM [76].

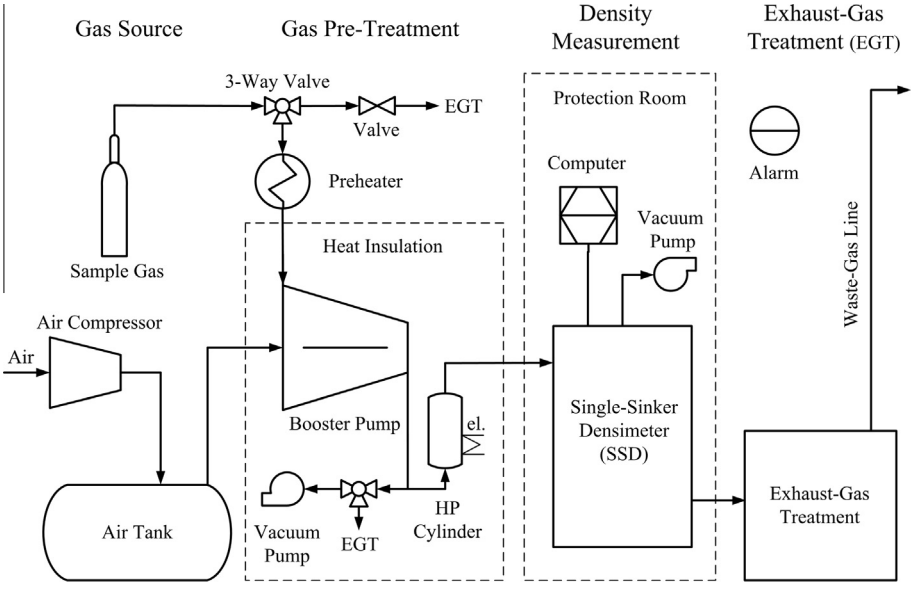

FIGURE 1. Density measurement system.

thermostat stages comprised a ring thermostat and a copper radiation shield. The temperature of the inner thermostat stage was controlled by means of electrical heating, whereas thermostating liquid was used for the outer thermostat stage. The main temperature measurement was conducted with a calibrated 25 Ω platinum resistance thermometer (PRT). A precision AC resistance

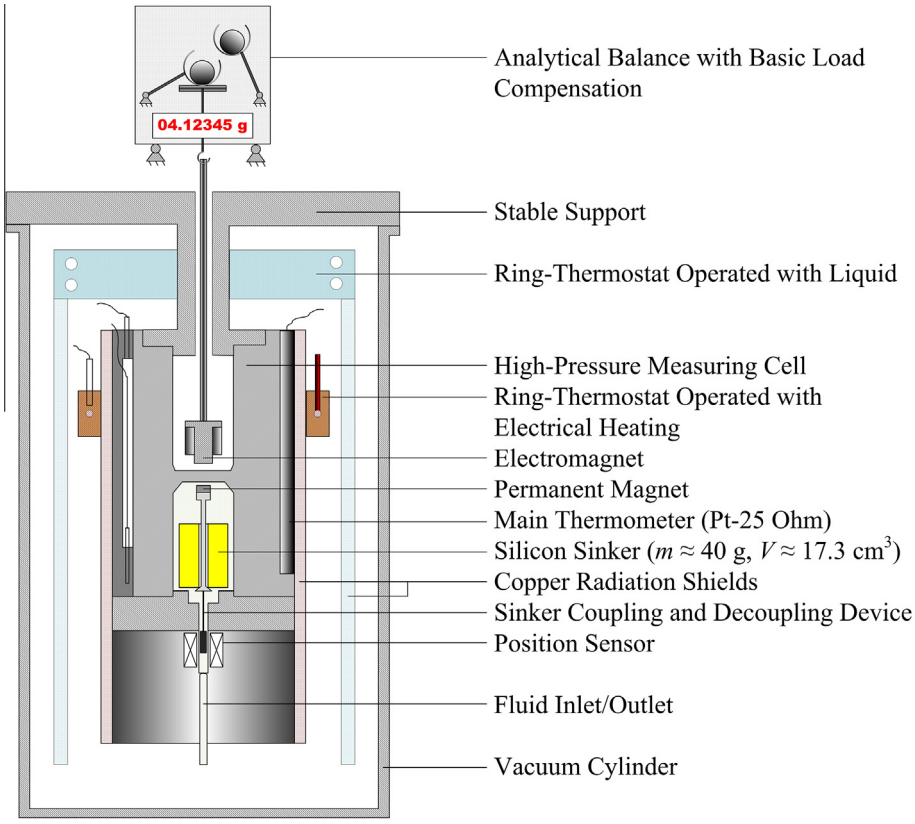

FIGURE 2. Schematic diagram of the single-sinker densimeter.

thermometry bridge (type: F700, ASL, UK) was used to measure the resistance of the main thermometer in reference to the calibrated bridge internal resistor. Pressures were measured up to 35 MPa with a calibrated Digiquartz intelligent pressure transmitter (type: 9000-6k-101, Paroscientific, USA). To measure the density of a gas sample, the sinker made of monocrystalline silicon ($V \approx 17.3$ cm^3, $m \approx 40.0$ g, $\rho \approx 2.31$ g/cm^3) was weighed inside the high-pressure measuring cell with an analytical balance (type: XP205, Mettler Toledo, Switzerland). The cell was made of beryllium copper with low magnetic susceptibility. This was essential for the use of the magnetic suspension coupling, which consisted of an electromagnet, a permanent magnet, a vertical position sensor, and an electronic position-control unit.

To yield the density of the fluid under study, the sinker was weighed twice, *i.e.*, m_{vac} when the measuring cell was evacuated and m_{fliud} when the cell was filled with fluid at pressure p and temperature T. With this, the density ρ was calculated by

$$\rho(T,p) = \frac{m_{vac}(T) - m_{fluid}(T,p)}{V_{sinker}(T,p)}, \tag{1}$$

where $V_{sinker}(T,p)$ is the volume of the sinker. The impact of changes in temperature and in pressure on the volume of the sinker is significant. *E.g.*, the relative changes in the value of V_{sinker} are 0.117% for the temperature range from T_0 to $T = 423.15$ K at constant pressure p_0 and −0.031% for the pressure range from p_0 to $p = 31.0$ MPa at constant temperature T_0. Thus, the sinker volume is corrected depending on temperature and pressure by

$$V_{sinker}(T,p) = V_0 \cdot \left[1 + 3 \cdot \overline{\alpha}|_{T_0}^{T} \cdot (T - T_0) - \frac{1}{K(T)} \cdot (p - p_0)\right]. \tag{2}$$

In equation (2) V_0 is the volume of the sinker at reference state ($p_0 = 0.10135$ MPa and $T_0 = 293.15$ K), $\overline{\alpha}|_{T_0}^{T}$ is the average value of the linear thermal expansion coefficient $\alpha(T)$ in the temperature range from T_0 to T, and $K(T)$ is the isothermal compression modulus. $\alpha(T)$ for monocrystalline silicon in the temperature range from (293 to 1000) K was given by Watanabe *et al.* [77] with the uncertainty impact on the value of V_{sinker} being less than 7 ppm in the temperature range from (298.15 to 423.15) K. $K(T)$ was calculated by

$$K(T) = \frac{c_{11}(T) + 2 \cdot c_{12}(T)}{3}, \tag{3}$$

where $c_{11}(T)$ and $c_{12}(T)$ are elastic moduli, values of which were obtained from [78,79].

2.2. Experimental procedures

Before starting measurements on a new gas sample, first the SSD and the gas pre-treatment section were evacuated for at least 30 min. Then the gas pre-treatment section was flushed with the new gas sample for about 1 min and filled to $p = 0.5$ MPa; the sample remained in the gas pre-treatment section for 5 min; then this section was evacuated for 5 min; this procedure was repeated three times. Afterwards the booster pump was used to fill the HP cylinder with the new gas sample. The HP cylinder was temperature controlled at approximately $T = 313.15$ K during the filling procedure. However, for pure carbon dioxide and mixtures with high carbon dioxide concentration, the pressure in the HP cylinder could not exceed 34 MPa due to technical reasons with our equipment. To solve this problem, the temperature of the HP cylinder was increased to achieve the designated pressure. The procedure of filling the HP cylinder took several hours; therefore, in the meantime, the SSD was filled with the new gas sample to $p = 0.5$ MPa; the sample remained inside the cell for 10 min; the cell was then evacuated for 10 min; this procedure was repeated three times. After that, the SSD was evacuated, and the

temperature was adjusted and controlled to the designated temperature. Following the filling procedure, the connection between the HP cylinder and the booster pump was shut off, and the gas on the booster pump side was released to reduce the risk of condensation and for safety reasons. Due to sample consumption, the pressure in the HP cylinder decreased during density measurement, which was compensated for by increasing the temperature of the HP cylinder.

Once the SSD and the gas pre-treatment section reached thermal equilibrium, measurements could be conducted. The SSD automatically acquired fluid from the HP cylinder via the gas-dosing system. On each isotherm, at first m_{vac} was determined in the evacuated measuring cell followed by m_{fliud} measurements in a pressure increasing fashion, *i.e.*, $p = (11.0, 13.0 \ldots$ to 31.0) MPa. Density measurements on nitrogen also included a series with decreasing pressures. In each (T,p) state point, 40 weighing cycles were conducted to obtain an average value.

The mixture composition could vary due to sorption effects inside the measuring cell [80]. The consequence is a change of the measured fluid density. Richter and Kleinrahm [80] suggested to investigate sorption effects in apparatuses used for thermophysical property measurements and to flush the measuring cell with fresh gas sample in order to reduce the distortion of density determination due to sorption effects. However, in the present work these effects were not investigated. Since flushing the measuring cell was not possible with our densimeter, we applied a purging procedure as previously described in this section. Nevertheless, sorption effects were probably small for our measurements because we measured far away from the dew line and our gas samples contained only small amounts of carbon dioxide. For future measurements with mixtures containing higher amounts of carbon dioxide possible sorption effects need to be considered.

2.3. Gas samples

The gas samples were all purchased from Beijing Beiwen Gas Company, China. The pure substances are specified in table 3. The binary mixtures were prepared gravimetrically by the supplier and the reported expanded uncertainties ($k = 2$) in composition were 0.001 mol fraction.

3. Uncertainty analysis

This section provides a detailed uncertainty analysis for the new SSD. The combined uncertainty of each measurement parameter (temperature, pressure, density, force transmission error (FTE) of the magnetic suspension coupling, and composition) is calculated according to the error propagation principle suggested by the Guide to the Expression of Uncertainty in Measurement (GUM) [76]. For our considerations we assume that the contributors to uncertainty are independent from each other.

3.1. Temperature uncertainty

The uncertainty budget for temperature measurement is summarized in table 4. The divisors in table 4 refer to GUM [76]. The main contributors to the uncertainty in temperature are the calibration, the drift of the thermometer, the temperature gradient along the wall of the measuring cell, and temperature oscillations over the measurement time.

For the main temperature measurement, the 25 Ω PRT and the AC resistance thermometry bridge including the connection wires were calibrated at the National Institute of Metrology, China (NIM). The calibration was done by simultaneously measuring the temperature in a thermal bath with our thermometer and a standard PRT of NIM. Our temperature measurement chain was calibrated over the temperature range from (273.15 to 423.15) K with temperature intervals of 25 K. Readings of the reference temperature measurement chain of NIM (T_{ref}) and resistance ratio readings of our thermometry bridge (r_{F700}) were correlated to

$$r_{F700} = r_0 \cdot \left(1 + a \cdot T_{ref} + b \cdot T_{ref}^2\right). \quad (4)$$

The maximum deviation of T_{ref} from values calculated with the correlation function was 2.9 mK. In our density measurement, with the readings of the thermometry bridge known, temperatures were directly determined by solving equation (4) using the fitted parameters r_0, a, and b. The standard uncertainty of the reference measurement chain of NIM over the temperature range from (273.15 to 423.15) K was reported by NIM to be 8.0 mK. However, other uncertainty contributions should be taken into consideration, such as the correlation function, self-heating of the sensor, heat dissipation of the test leads, temperature gradient in the thermal bath, *etc.* To be conservative, the standard uncertainty of the calibration of our main temperature measurement chain was estimated to be 16.0 mK.

The uncertainty of the value for the internal reference resistor of the thermometry bridge was taken into account within the calibration. However, the drift of the internal reference resistor needs to be considered. According to the manufacturer's specifications, the long-term stability of the resistor is better than 1 ppm/month, which corresponds to a maximum of 0.4 mK/month for our measurements. Our main temperature measurement chain is calibrated once a year and we carried out the present measurements within 6 months after the latest calibration. Therefore, 6 months were considered to calculate the uncertainty of the drift given in table 4.

TABLE 4
Uncertainty budgets.

Contributors	Estimated uncertainty	Divisor	Contribution
Temperature measurement (mK)			
Calibration	16.0	1	16.0
Drift	2.4	$\sqrt{3}$	1.4
Temperature gradient	20.0	$2\sqrt{3}$	5.8
Oscillation	4.0	1	4.0
Combined uncertainty			17.5
Expanded uncertainty ($k = 2$)			35.0
Pressure measurement (kPa)			
Calibration	2.66	2	1.33
Drift	2.10	2	1.05
Combined uncertainty			1.69
Expanded uncertainty ($k = 2$)			3.39

TABLE 3
Sample information.

Chemical name	Source	Purification method	Purity/mole fraction	Analysis method
Argon	Beijing Beiwen Gas	None	0.999999	Gas chromatography
Nitrogen	Beijing Beiwen Gas	None	0.999999	Gas chromatography
Carbon dioxide	Beijing Beiwen Gas	None	0.999995	Gas chromatography

The 25 Ω PRT was contacted to the measuring cell by means of a thermometer well made from copper. The probe tip was located near the bottom of the cell. Although the cell is a cylinder with an axisymmetric structure and an environment of almost constant temperature, a temperature gradient needs to be considered. Therefore, we took a temperature difference between the fluid in the cell and the probe tip of the PRT as well as an improvable contacting of PRT and cell into account. The temperature gradient at the highest temperature 423.15 K was estimated to be less than 20 mK.

The temperature of the measuring cell was controlled by a two-stage thermostat surrounding the cell (see Section 2.1 and figure 2). The outer stage was controlled at a temperature 10 K below the cell temperature, while the inner stage being closely attached to the cell was heated to the target temperature. Temperature oscillations over time were statistically calculated during measurement from 2 mK at $T = 298.15$ K to 4 mK at $T = 423.15$ K.

In summary, the combined expanded uncertainty ($k = 2$) of the main temperature measurement was 35 mK. To reduce this uncertainty in the future, the calibration could be carried out on ITS-90 by use of fixed-point cells, an external standard resistor with only a small drift over time could be implemented, and the temperature gradient could be reduced by improving the contacting of PRT, thermometer well, and measuring cell.

3.2. Pressure uncertainty

The uncertainty budget for pressure measurement is summarized in table 4. The Digiquartz intelligent pressure transmitter was calibrated using a high-pressure gas-piston gauge (HGPG) at Beijing Aerospace Institute for Metrology and Measurement Technology, China. The calibration was conducted in three cycles, each of which consisted of one pressure-increasing procedure and one pressure-decreasing procedure. The deviations of pressures measured with our pressure transmitter from values measured with the HGPG were systematical and smaller than 1.0 kPa over the pressure range from (11 to 31) MPa. A correlation function between the deviations and the readings of the HGPG was fitted. This function was adopted to adjust our pressure measurement mathematically, instead of changing calibration parameters in the transmitter. According to the calibration certificate, the combined expanded uncertainty ($k = 2$) of the pressure measurement with the transmitter was 2.66 kPa. Given the manufacturer's specifications, the pressure transmitter has excellent stability with a maximum drift of 0.005% ($k = 2$) of full scale per year. The transmitter is calibrated once every 2 years, and our measurements were carried out within 12 months after the latest calibration. Therefore, 12 months were applied to calculate the uncertainty of the drift stated in table 4.

The altitude difference between the measuring cell and the pressure transmitter was approximately 41 cm, therefore, a hydrostatic pressure correction should be taken into consideration. For example, for pure nitrogen, the correction in density measurement due to hydrostatic pressure ranges from 0.0049% at $p = 11$ MPa to 0.0022% at $p = 31$ MPa. We simply applied this pressure correction, which is therefore not included in the measurement uncertainty. In summary, the combined expanded uncertainty ($k = 2$) of the pressure measurement was 3.39 kPa.

3.3. Density uncertainty

According to equation (1), the uncertainty in density measurement was basically determined by the uncertainties of the sinker weighings (in the evacuated measuring cell and in the fluid under study) and of the volume of the sinker. As described in Section 2, the sinker weighings were carried out utilizing a magnetic-suspension balance (MSB) with a combined expanded uncertainty ($k = 2$) of 0.002% of the balance reading (as stated by Rubotherm). The volume of the sinker V_0 at reference state ($p_0 = 0.10135$ MPa and $T_0 = 293.15$ K) was first calibrated by Center for Measurement and Calibration GmbH in Germany with an expanded uncertainty ($k = 2$) of 0.006 cm^3 or 0.035%. The uncertainty of the sinker volume is subject for improvement in future work.

To reduce the uncertainty of V_0 for the present work, a method was proposed to re-determine the volume of the sinker using the SSD itself without removing the sinker from the measuring cell. Pure nitrogen was measured at three temperatures (298.15, 348.15, and 398.15) K and three pressures (25, 27, and 29) MPa, where the relative uncertainty of pressure measurement was small. Each isotherm was measured twice by performing one pressure-increasing procedure and one pressure-decreasing procedure. The optimized V_0 was determined by minimizing the following target function

$$f = \sum_{i}^{\text{All thermal states}} \left\{ \frac{m_{\text{vac}} - m_{\text{fluid},i}}{V_{\text{sinker}}(V_0, T_i, p_i)} - \rho_{\text{EOS}}(T_i, p_i) \right\}^2, \tag{5}$$

where $\rho_{\text{EOS}}(T,p)$ was obtained from the reference EOS developed by Span *et al.* [1]. The optimized result was 17.318 cm^3 and the uncertainty of this value was estimated as follows.

The uncertainty of the EOS $u(\rho_{\text{EOS}})/\rho_{\text{EOS}}$ in the relevant measuring range is 0.02% ($k = 2$) [1]. The combined uncertainty of $\rho_{\text{EOS}}(T,p)$ (including the uncertainties of temperature and pressure measurement) was calculated by

$$\left(\frac{u(\rho_{\text{EOS}}(T,p))}{\rho_{\text{EOS}}(T,p)}\right)^2 = \left(\frac{u(\rho_{\text{EOS}})}{\rho_{\text{EOS}}}\right)^2 + \left(\frac{\partial\rho}{\partial T}\cdot\frac{u(T)}{T}\right)^2 + \left(\frac{\partial\rho}{\partial p}\cdot\frac{u(p)}{p}\right)^2, \tag{6}$$

where the partial derivatives were estimated with the reference EOS. Then, the combined expanded uncertainty ($k = 2$) of V_0 was determined by applying the error propagation principle to the following equations:

$$V_{\text{sinker}}(T_i, p_i) = \frac{m_{\text{vac}} - m_{\text{fluid},i}}{\rho_{\text{EOS}}(T_i, p_i)}, \tag{7}$$

$$V_0 = \frac{V_{\text{sinker}}(T,p)}{1 + 3\cdot\overline{\alpha}|_{T_0}^{T}\cdot(T - T_0) - \frac{1}{K(T)}\cdot(p - p_0)}. \tag{8}$$

The result was 0.0045 cm^3. The old value and the new value of V_0 agree with each other within their respective uncertainties.

After the new value of V_0 and its uncertainty were determined, the combined expanded ($k = 2$) uncertainty in density measurement was calculated by employing the error propagation principle to equations (1) and (2), and the result was 0.026%. However, as it will be described in Section 4.1, a correction function was applied to the experimental density; this correction function was set up based on the state-of-the-art nitrogen EOS [1]; therefore, the uncertainty of this EOS 0.02% ($k = 2$) had to be considered. In summary, the combined expanded uncertainty of the density measurement was 0.033% ($k = 2$).

3.4. Consideration of the force transmission error (FTE)

For highly accurate density measurements with a MSB, the FTE needs to be taken into consideration. The FTE is an inevitable error in the MSB because the material of the pressure cell and the sample fluid itself are not magnetically neutral. The magnetic properties of the pressure cell and the sample fluid will exert magnetic forces on the magnetic-suspension coupling, thus distorting the weighing result.

The FTE caused by magnetic properties of the pressure cell is unique for each individual apparatus. Kuramoto *et al.* [22] estimated a relative systematic error of 0.7 ppm in the density determination caused by the magnetic properties of their pressure cell. The pressure cell of their apparatus was made of a copper-chrome-zirconium alloy and was designed to work at pressures up to 20 MPa. McLinden *et al.* [81] determined an impact of 20 ppm on density measurement from the magnetic properties of the pressure cell. The SSD they studied was installed at Ruhr-University Bochum and is now dismantled. The design of the pressure cell of this SSD was different from ours. The pressure cell was made of stainless steel and the coupling housing was made of copper-beryllium alloy. This system was designed for pressures up to 30 MPa. Cristancho *et al.* [82] determined the FTE caused by the magnetic properties of their pressure cell to be approximately 189 ppm, with the pressure cell made of a copper-beryllium alloy designed for pressures up to 200 MPa. To resist higher pressures, the pressure-separating wall of the measuring cell becomes thicker. With an increasing wall thickness the FTE becomes larger. The pressure cell of our apparatus was made of copper-beryllium and designed to work at pressures up to 35 MPa, which is somewhat similar to the apparatus at Ruhr-University Bochum [81]. Therefore, the FTE of the pressure cell of our apparatus was roughly estimated to be 20 ppm.

The FTE caused by the magnetic properties of the fluid does not only depend on the fluid itself, but also on the individual apparatus. In this context especially the alignment of the permanent magnet, the pressure cell, and the electromagnet [83,84] is of importance. According to Rubotherm's specification for the MSB, the fluid specific FTE for the fluids of our interest, such as nitrogen, argon, and carbon dioxide, is in the order of 50 ppm. A preliminary empirical correlation equation was established by Klimeck [85] to estimate the uncertainty contribution from the magnetic properties of the fluid

$$\varepsilon_\rho = \left(\frac{\Delta\rho}{\rho}\right) \approx M_C \cdot \frac{-\chi_S}{10^{-8}\ \mathrm{m^3}\ \cdot\ \mathrm{kg^{-1}}}, \tag{9}$$

where M_C is the individual apparatus constant; $\chi_S = \chi/\rho$ is the specific magnetic susceptibility and χ is the magnetic susceptibility of the sample fluid. As discussed in this section before, our apparatus had a certain similarity to the one at Ruhr-University Bochum; therefore, we roughly assumed that our MSB had a similar value of M_C as theirs, which is $80 \cdot 10^{-6}$. According to equation (9), taking nitrogen ($\chi_S = -0.54 \cdot 10^{-8}\ \mathrm{m^3 \cdot kg^{-1}}$) as an example, the maximum possible ε_ρ is +44 ppm, which agrees with Rubotherm's specification. A comprehensive analysis of the FTE of our apparatus using the state-of-the-art method published by McLinden *et al.* [81] will be part of future work.

3.5. Sample composition uncertainty

The expanded uncertainty ($k = 2$) of the sample composition was stated by the supplier to be 0.001 mol fraction for each component. A sensitivity analysis using the GERG-2008 EOS yielded a contribution of 0.10% to the combined expanded uncertainty ($k = 2$) in density for the (nitrogen + carbon dioxide) mixtures and 0.05% to the combined expanded uncertainty ($k = 2$) in density for the (argon + carbon dioxide) mixtures. Although we did not carry out extensive tests, it is likely that sorption effects as described by Richter and Kleinrahm [80] were not significant for our measurements since we measured far away from the dew line and our gas samples contained only small amounts of carbon dioxide. However, we still account 0.1% for the contribution from sorption effects to the uncertainty in density measurement due to our densimeter filling procedure with a booster pump and the use of a HP cylinder, which is not electropolished from the inside. Moreover, the setup of our system is quite complex, and whilst we were very mindful with the sample handling, we cannot rule out the possibility of condensation in very few and small spots of the system. Furthermore, due to the fact that we do not have the capability to flush our density measuring system changes in composition might have occurred.

3.6. Combined uncertainty in density

In summary, taking the uncertainties in temperature, pressure, and density measurements as well as the FTE into consideration, the relative combined expanded uncertainty ($k = 2$) in density for measurements on pure substances ranged from 0.046% at $p = 11$ MPa to 0.036% at $p = 31$ MPa. The relative combined expanded uncertainty ($k = 2$) in density was 0.15% for the (nitrogen + carbon dioxide) mixtures and 0.12% for the (argon + carbon dioxide) mixtures, with the composition uncertainty as the main contributor.

4. Results

4.1. Results from commissioning the new single-sinker densimeter

Within the scope of commissioning the new SSD, measurements on three pure substances were carried out: nitrogen, at $T = (298.15, 348.15, \text{and } 398.15)$ K with pressures up to 33 MPa; argon, at $T = (298.15, 348.15, \text{and } 398.15)$ K with pressures up to 33 MPa; carbon dioxide, at $T = 323.15$ K with pressures up to 29 MPa. The relative deviation σ_r, is defined by

$$\sigma_r = 100 \cdot \frac{\rho_{\mathrm{exp}} - \rho_{\mathrm{EOS}}}{\rho_{\mathrm{EOS}}}, \tag{10}$$

where ρ_{exp} is the experimental density, and ρ_{EOS} is the respective value calculated with the state-of-the-art EOS (nitrogen [1], argon [2], and carbon dioxide [3]). The results of the measurements on the pure substances are shown in the left column of figure 3. For clarity error bars for the relative combined expanded uncertainty ($k = 2$) in density measurement are illustrated only for the measurements on carbon dioxide. Our experimental densities agree with the EOS within their uncertainties; nonetheless, in some cases, they exceed the uncertainty bounds of the EOS, *i.e.*, ±0.02% for nitrogen [1], ±0.03% for argon [2], and ±0.03% for carbon dioxide [3]. For all three substances similar pressure and temperature dependent systematic relative deviations were observed. The reason for the behavior of the experimental data could not be fully clarified within the present work. However, to compensate for the systematic deviation, which was probably related to pressure measurement, to the determination of the sinker volume and to the FTE, a correction function based merely on the nitrogen measurements was applied. The original experimental data from our measurements on nitrogen were used to calculate $\delta(T,p)$ by

$$\delta(T,p) = \left(\frac{\rho_{\mathrm{EOS}}(T,p)}{\rho_{\mathrm{exp}}(T,p)} - 1\right) \cdot 100. \tag{11}$$

Then parameters $n_{p,i}$ and $n_{T,i}$ in the following equation

$$\delta(T,p) = \left(\sum_{i=0}^{4} n_{p,i} \cdot p^i\right) \cdot \left(\sum_{i=0}^{1} n_{T,i} \cdot T^i\right). \tag{12}$$

were fitted. Equation (12) with the determined parameters $n_{p,i}$ and $n_{T,i}$ was used as the correction function and the original experimental density data were corrected by

$$\rho_{\mathrm{exp,cor}}(T,p) = \rho_{\mathrm{exp}}(T,p) \cdot [\delta(T,p)/100 + 1]. \tag{13}$$

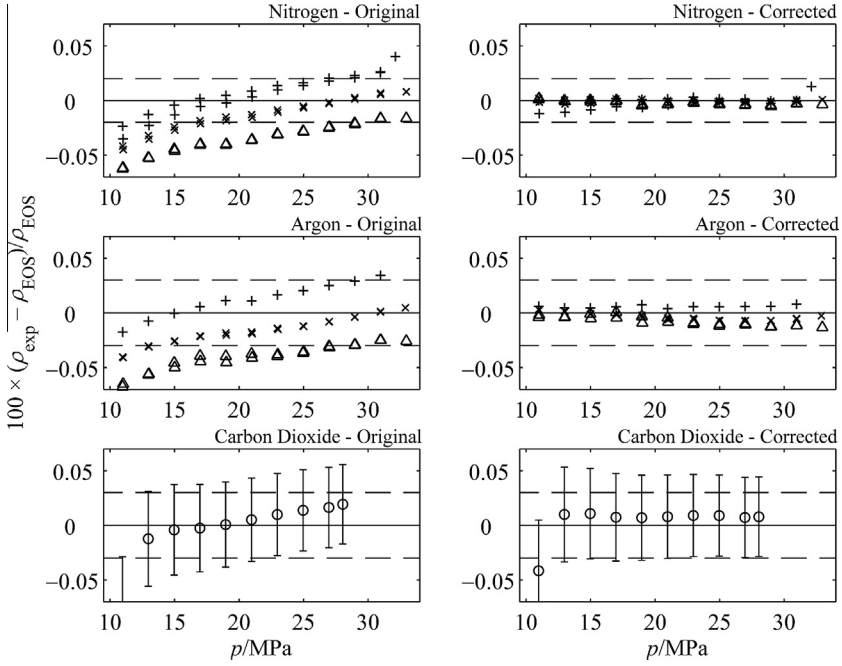

FIGURE 3. Relative deviations of experimental densities ρ_{exp} for nitrogen, argon, and carbon dioxide from densities ρ_{EOS} calculated with the respective reference equations of state [1–3]. Left: results when using the densimeter as an absolute device; Right: results after applying the correction function, equation (12), to the original density data. +, T = 298.15 K; ○, T = 323.15 K; ×, T = 348.15 K; △, T = 398.15 K; dashed line, uncertainty bounds of the respective reference equation of state. For clarity error bars for the combined expanded density measurement uncertainty (k = 2) are illustrated only for the measurements on carbon dioxide.

TABLE 5
Experimental values of density ρ at temperature T and pressure p on pure substances.

T/K	p/MPa	ρ/kg · m^{-3}	T/K	p/MPa	ρ/kg · m^{-3}	T/K	p/MPa	ρ/kg · m^{-3}	T/K	p/MPa	ρ/kg · m^{-3}
Nitrogen (with purity 0.999999 mol fraction)											
298.234	10.976	123.118	298.241	21.004	223.219	348.231	32.959	269.893	398.251	22.969	174.806
298.233	12.976	144.452	298.233	19.010	204.785	348.247	30.963	257.258	398.262	24.969	187.737
298.236	14.976	165.170	298.239	17.014	185.557	348.235	28.967	244.162	398.235	26.967	200.287
298.228	16.971	185.161	298.245	15.014	165.544	348.248	26.979	230.612	398.244	28.966	212.445
298.242	18.975	204.467	298.235	13.017	144.868	348.291	25.001	216.612	398.260	30.962	224.219
298.231	20.970	222.928	298.237	11.019	123.569	348.279	23.006	202.007	398.219	32.961	235.672
298.231	22.971	240.653	348.254	10.981	103.086	348.275	21.013	186.886	398.270	30.977	224.298
298.235	24.970	257.550	348.282	12.976	120.712	348.279	19.011	171.174	398.222	28.993	212.616
298.232	26.968	273.675	348.282	14.976	137.928	348.232	17.010	154.974	398.214	27.000	200.503
298.228	28.965	289.039	348.258	16.972	154.648	348.256	15.015	138.272	398.233	25.002	187.957
298.218	30.959	303.674	348.237	18.974	170.907	348.246	13.016	121.065	398.187	23.005	175.071
298.117	32.109	311.953	348.259	20.971	186.577	348.272	11.019	103.420	398.169	21.012	161.802
298.331	30.945	303.445	348.253	22.970	201.759	398.253	12.976	104.354	398.222	19.011	148.062
298.234	28.966	289.035	348.247	24.970	216.421	398.279	14.977	119.222	398.362	17.012	133.928
298.232	26.969	273.679	348.240	26.968	230.548	398.292	16.973	133.670	398.389	15.006	119.391
298.244	24.971	257.546	348.214	28.966	244.176	398.283	18.975	147.786	398.299	13.014	104.623
298.237	22.992	240.817	348.255	30.963	257.253	398.241	20.972	161.499	398.324	11.005	89.328
Argon (with purity 0.999999 mol fraction)											
298.230	10.975	185.811	348.241	16.969	235.508	348.260	21.009	288.719	398.284	28.964	329.330
298.230	12.977	220.515	348.216	18.971	262.184	348.212	19.007	262.654	398.225	30.962	349.179
298.227	14.975	254.862	348.273	20.969	288.199	348.232	17.005	236.000	398.207	32.960	368.494
298.239	16.973	288.723	348.266	22.970	313.733	348.243	15.014	209.051	398.189	30.985	349.444
298.225	18.968	321.888	348.261	24.967	338.568	348.278	13.012	181.556	398.202	28.999	329.764
298.227	20.970	354.268	348.237	26.966	362.782	348.280	11.019	153.917	398.346	27.004	309.394
298.228	22.969	385.599	348.211	28.963	386.293	397.907	12.975	155.101	398.471	25.004	288.536
298.226	24.967	415.802	348.194	30.960	409.077	397.977	14.981	178.323	398.258	23.005	267.500
298.223	26.965	444.810	348.252	32.887	430.274	398.167	16.979	201.050	398.252	21.010	245.897
298.221	28.963	472.591	348.243	30.961	409.019	398.605	18.975	223.208	398.238	19.010	223.818
298.205	30.957	499.118	348.224	28.964	386.289	398.868	20.975	245.092	398.296	17.005	201.261
348.210	10.976	153.363	348.273	26.989	363.019	398.915	22.970	266.619	398.310	15.013	178.513
348.252	12.974	181.049	348.282	25.000	338.949	398.096	24.969	288.472	398.262	13.011	155.367
348.274	14.970	208.427	348.287	23.010	314.199	398.227	26.971	309.171	398.243	11.017	132.022
Carbon dioxide (with purity 0.999995 mol fraction)											
323.204	10.968	497.981	323.250	16.965	739.597	323.248	22.962	815.681	323.247	28.037	856.967
323.246	12.967	633.580	323.239	18.962	770.445	323.241	24.961	833.514			
323.237	14.966	698.200	323.259	20.966	795.018	323.247	26.959	849.181			

The combined expanded uncertainties (k = 2) in measurements are 35 mK for temperature, 3.39 kPa for pressure, and 0.033% for density. The pure substances are all in supercritical state.

TABLE 6
Experimental values of density ρ at temperature T and pressure p on binary mixtures.

T/K	p/MPa	ρ/kg · m^{-3}	T/K	p/MPa	ρ/kg · m^{-3}	T/K	p/MPa	ρ/kg · m^{-3}	T/K	p/MPa	ρ/kg · m^{-3}
0.95 N_2 + 0.05 CO_2			0.99 N_2 + 0.01 CO_2			0.95 Ar + 0.05 CO_2			0.99 Ar + 0.01 CO_2		
298.184	10.974	128.536	298.189	10.975	124.200	298.222	10.976	190.182	298.194	10.975	187.045
298.187	12.974	151.108	298.189	12.977	145.801	298.227	12.976	226.201	298.195	12.973	222.038
298.192	14.973	173.056	298.189	14.975	166.746	298.229	14.974	261.987	298.191	14.969	256.759
298.187	16.968	194.247	298.189	16.973	186.990	298.226	16.969	297.274	298.190	16.969	291.075
298.188	18.971	214.733	298.189	18.971	206.482	298.228	18.970	331.923	298.193	18.969	324.674
298.189	20.972	234.340	298.187	20.971	225.196	298.228	20.969	365.576	298.197	20.967	357.351
298.186	22.968	253.055	298.190	22.969	243.092	298.233	22.968	398.090	298.197	22.966	389.003
298.194	24.966	270.906	298.189	24.967	260.186	298.229	24.967	429.349	298.199	24.964	419.491
298.185	26.964	287.919	298.183	26.965	276.485	298.227	26.965	459.226	298.195	26.962	448.747
298.177	28.960	304.080	298.183	28.960	291.991	298.225	28.963	487.701	298.178	28.957	476.725
298.111	30.854	318.784	298.153	30.889	306.308	298.174	30.944	514.698	298.123	30.871	502.471
323.183	10.979	116.684	323.207	10.980	112.998	323.256	10.976	170.993	323.202	10.978	168.714
323.189	12.977	136.963	323.202	12.978	132.477	323.257	12.974	202.641	323.218	12.973	199.627
323.176	14.973	156.725	323.188	14.974	151.425	323.257	14.973	234.077	323.213	14.970	230.302
323.204	16.971	175.903	323.196	16.973	169.822	323.255	16.970	265.100	323.207	16.971	260.652
323.201	18.972	194.494	323.205	18.975	187.629	323.266	18.969	295.579	323.211	18.969	290.390
323.188	20.974	212.443	323.204	20.974	204.784	323.271	20.973	325.456	323.213	20.969	319.490
323.192	22.968	229.628	323.198	22.971	221.285	323.252	22.969	354.460	323.215	22.966	347.807
323.195	24.967	246.174	323.192	24.968	237.145	323.239	24.968	382.594	323.199	24.965	375.340
323.197	26.964	262.031	323.189	26.966	252.374	323.271	26.965	409.680	323.210	26.962	401.924
323.195	28.961	277.225	323.181	28.962	266.975	323.253	28.963	435.856	323.212	28.960	427.589
323.179	30.957	291.768	323.180	30.957	280.954	323.237	30.958	460.997	323.197	30.955	452.317
348.174	10.975	107.020	348.167	10.975	103.828	348.297	10.979	155.900	348.252	10.977	154.064
348.161	12.976	125.560	348.176	12.974	121.664	348.299	12.976	184.300	348.245	12.974	181.967
348.154	14.974	143.613	348.204	14.978	139.081	348.302	14.972	212.437	348.213	14.972	209.619
348.194	16.972	161.157	348.211	16.969	155.902	348.300	16.971	240.266	348.210	16.970	236.897
348.219	18.976	178.236	348.192	18.968	172.299	348.277	18.972	267.685	348.209	18.972	263.764
348.226	20.969	194.689	348.180	20.972	188.207	348.277	20.972	294.530	348.217	20.972	290.057
348.207	22.970	210.667	348.202	22.973	203.544	348.293	22.970	320.729	348.257	22.968	315.675
348.207	24.968	226.054	348.177	24.966	218.313	348.306	24.969	346.237	348.254	24.966	340.708
348.201	26.965	240.883	348.160	26.965	232.594	348.294	26.966	371.043	348.242	26.963	365.062
348.236	28.961	255.123	348.164	28.963	246.335	348.280	28.962	395.094	348.233	28.960	388.704
348.195	30.958	268.893	348.176	30.959	259.551	348.250	30.958	418.385	348.224	30.956	411.615
373.141	10.975	99.052	373.143	10.978	96.257	373.242	10.977	143.580	373.248	10.978	142.110
373.168	12.975	116.113	373.174	12.978	112.737	373.302	12.975	169.447	373.249	12.977	167.627
373.111	14.975	132.811	373.181	14.973	128.781	373.315	14.971	195.043	373.240	14.972	192.822
373.179	16.969	148.990	373.204	16.976	144.455	373.289	16.972	220.418	373.217	16.970	217.712
373.194	18.968	164.767	373.198	18.972	159.653	373.281	18.969	245.312	373.219	18.968	242.204
373.162	20.970	180.142	373.208	20.974	174.438	373.311	20.969	269.779	373.238	20.969	266.255
373.195	22.970	194.991	373.196	22.969	188.731	373.319	22.966	293.716	373.227	22.970	289.853
373.190	24.968	209.378	373.144	24.968	202.615	373.322	24.968	317.167	373.226	24.965	312.835
373.192	26.966	223.295	373.142	26.966	216.025	373.311	26.966	340.003	373.229	26.964	335.305
373.200	28.961	236.723	373.161	28.962	228.969	373.292	28.963	362.242	373.237	28.960	357.169
373.171	30.957	249.734	373.185	30.958	241.480	373.288	30.959	383.847	373.223	30.957	378.472
398.118	10.979	92.339	398.165	10.981	89.797	398.369	10.980	133.275	398.283	10.979	132.065
398.202	12.973	108.135	398.224	12.974	105.084	398.356	12.973	157.068	398.263	12.977	155.613
398.205	14.975	123.655	398.190	14.974	120.089	398.333	14.977	180.735	398.296	14.970	178.803
398.231	16.974	138.767	398.146	16.976	134.736	398.361	16.970	203.950	398.305	16.969	201.750
398.214	18.973	153.504	398.196	18.973	148.923	398.352	18.973	226.932	398.298	18.971	224.388
398.219	20.969	167.809	398.189	20.968	162.734	398.346	20.972	249.488	398.280	20.968	246.590
398.211	22.970	181.754	398.203	22.966	176.162	398.340	22.971	271.617	398.298	22.969	268.392
398.206	24.969	195.274	398.199	24.970	189.239	398.331	24.965	293.233	398.298	24.967	289.714
398.211	26.967	208.381	398.165	26.965	201.890	398.311	26.966	314.455	398.286	26.962	310.557
398.184	28.962	221.089	398.180	28.963	214.146	398.315	28.963	335.112	398.288	28.962	330.960
398.168	30.958	233.410	398.170	30.957	226.029	398.332	30.959	355.238	398.278	30.957	350.842
423.175	10.978	86.517	423.177	10.979	84.203	423.335	10.981	124.535	423.221	10.980	123.515
423.177	12.971	101.311	423.167	12.979	98.597	423.310	12.974	146.650	423.235	12.971	145.339
423.176	14.973	115.841	423.108	14.972	112.628	423.335	14.975	168.571	423.227	14.969	166.982
423.183	16.967	129.977	423.160	16.970	126.322	423.346	16.970	190.146	423.223	16.967	188.325
423.160	18.970	143.837	423.173	18.968	139.677	423.337	18.970	211.466	423.278	18.967	209.329
423.163	20.971	157.318	423.181	20.972	152.731	423.353	20.971	232.422	423.297	20.973	230.071
423.136	22.965	170.413	423.191	22.973	165.419	423.364	22.968	252.983	423.301	22.965	250.298
423.126	24.967	183.194	423.215	24.968	177.709	423.323	24.968	273.195	423.334	24.964	270.201
423.127	26.965	195.591	423.221	26.966	189.691	423.331	26.968	292.962	423.344	26.961	289.685
423.127	28.962	207.636	423.207	28.961	201.322	423.338	28.966	312.296	423.328	28.959	308.785
423.129	30.956	219.326	423.181	30.957	212.642	423.345	30.960	331.165	423.304	30.956	327.480

The relative combined expanded uncertainty (k = 2) in density was 0.15% for the (nitrogen + carbon dioxide) mixtures and 0.12% for the (argon + carbon dioxide) mixtures. The combined expanded uncertainties (k = 2) in measurements are 35 mK for temperature, 3.39 kPa for pressure, and 0.033% for density. The mixtures were prepared gravimetrically with the expanded uncertainties (k = 2) in composition of 0.001 mol fraction. The mixtures are all in supercritical state.

The corrected experimental (p,ρ,T) data of the three pure substances are listed in table 5. As shown in the right column of figure 3, the corrected experimental densities $\rho_{exp,cor}$ agree with the respective EOS within approximately 0.01% for all three pure substances. Only the data for carbon dioxide at $T = 323.15$ K and $p = 11$ MPa show a larger relative deviation. Although the correction function was only fitted to our experimental data for nitrogen, it worked well for all three pure substances. Thus, we concluded that the correction function was applicable for the data analysis of the mixture measurements with the main components being nitrogen and argon.

4.2. Results for the (nitrogen + carbon dioxide) mixtures

The (p,ρ,T,x) behavior of two (nitrogen + carbon dioxide) mixtures with the compositions (0.05 and 0.01) mole fraction carbon dioxide was investigated along six isotherms at $T = (298.15, 323.15, 348.15, 373.15, 398.15,$ and $423.15)$ K with pressures from (11 to 31) MPa. The results are listed in table 6, and relative deviations to the GERG-2008 EOS, as implemented in the NIST REFPROP database of Lemmon *et al.* [86], for the isothermal data are shown in figure 4. For clarity the error bar for the combined expanded uncertainty ($k = 2$) in density measurement is plotted only for one measurement point.

For the (0.95 nitrogen + 0.05 carbon dioxide) mixture, the experimental densities agree with the GERG-2008 EOS (zero line in figure 4) within 0.1%, which is also the uncertainty reported for the GERG-2008 EOS on this mixture for the respective conditions. Generally the relative deviations for the different isotherms increase with temperature and pressure. They all show similar trends. It is expected that deviations would decrease at lower pressures and would eventually converge to zero when approaching the ideal gas limit. As it can be seen in figure 4, the trend of the deviations with temperature and pressure agrees well with the experimental results for a (0.90 nitrogen + 0.10 carbon dioxide) mixture of Mondéjar *et al.* [35]. For example, at $T = 298.15$ K ($T = 300$ K in Mondéjar *et al.*), first both data sets show slightly decreasing deviations and then, from a turning point in the pressure range from (14 to 16) MPa, deviations increase with increasing pressure. This agreement suggests that the correction function, introduced in the previous section, improves the reliability of our data and is consistently applicable for the mixtures under study.

The agreement of the experimental densities for the (0.99 nitrogen + 0.01 carbon dioxide) mixture with GERG-2008 EOS is within 0.015%. The relative deviations are much smaller compared to the (0.95 nitrogen + 0.05 carbon dioxide) mixture; probably because of the smaller carbon dioxide concentration. Along all isotherms, the trend of the deviations with pressures is similar. In general relative deviations increase with increasing temperature, except at $T = 298.15$ K.

4.3. Results for the (argon + carbon dioxide) mixtures

We also investigated the (p,ρ,T,x) behavior of two (argon + carbon dioxide) mixtures with the compositions (0.05 and 0.01) mole fraction carbon dioxide along six isotherms at $T = (298.15, 323.15, 348.15, 373.15, 398.15,$ and $423.15)$ K with pressures from (11 to 31) MPa. The results are listed in table 6, and relative deviations from the GERG-2008 EOS for the isothermal data are shown in figure 5. The behavior of the EOS-CG [87,88], a new Helmholtz energy model for CCS mixtures as implemented in the TREND software package of Ruhr-University Bochum [89], is also plotted. However, in figure 5 the behavior of the EOS-CG is only plotted for $T = 423.15$ K because for temperatures from (298.15 to 423.15) K the behavior is similar to the GERG equation. As both equations contain the same binary specific departure function for the (nitrogen + carbon dioxide) mixture, the behavior of the

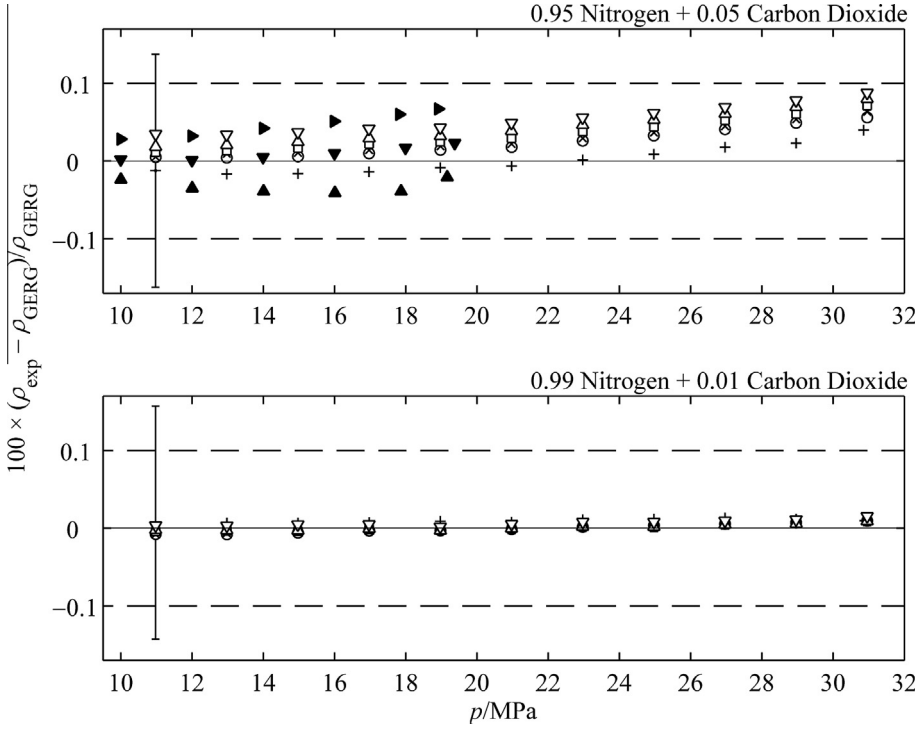

FIGURE 4. Relative deviations of experimental densities ρ_{exp} for (nitrogen + carbon dioxide) mixtures from densities ρ_{GERG} calculated by GERG-2008 EOS [13]. +, $T = 298.15$ K; ○, $T = 323.15$ K; ×, $T = 348.15$ K; □, $T = 373.15$ K; △, $T = 398.15$ K; and ▽, $T = 423.15$ K from our work; ▲, $T = 300$ K; ▼, $T = 350$ K; and ▶, $T = 400$ K on (0.90 nitrogen + 0.10 carbon dioxide) from Mondéjar *et al.* [35]; dashed line, uncertainty bounds of GERG-2008 EOS. For clarity the error bar for the combined expanded uncertainty ($k = 2$) in density measurement is plotted only for one measurement point.

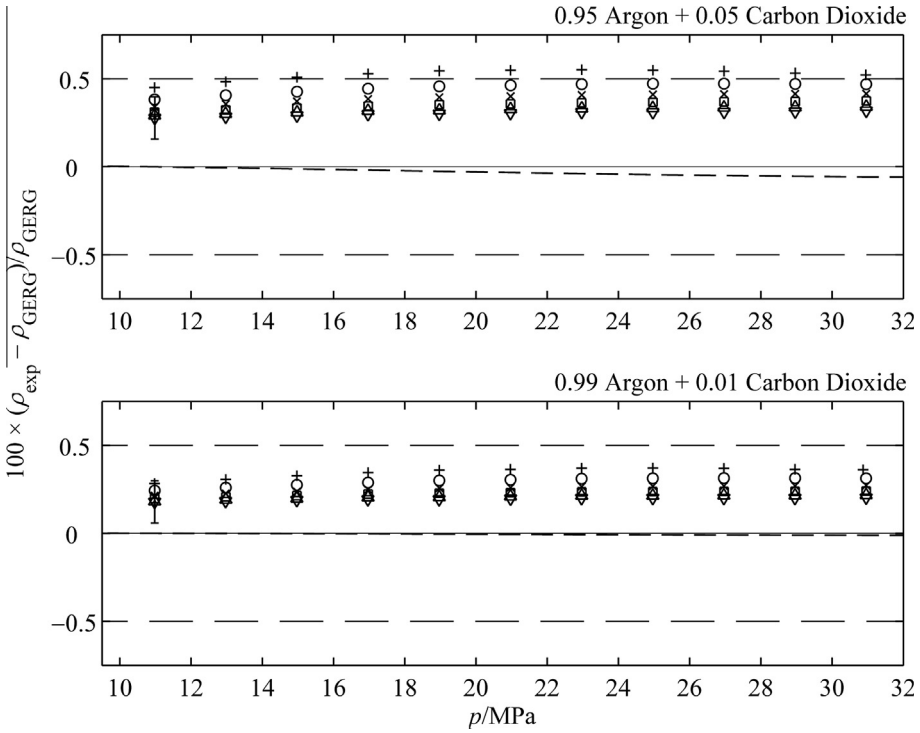

FIGURE 5. Relative deviations of experimental densities ρ_{exp} for (argon + carbon dioxide) mixtures from densities ρ_{GERG} calculated by GERG-2008 EOS [13]. +, T = 298.15 K; ○, T = 323.15 K; ×, T = 348.15 K; □, T = 373.15 K; △, T = 398.15 K; ▽, T = 423.15 K; long dashed line, uncertainty bounds of GERG-2008 EOS [13]; short dashed line, relative deviations of EOS-CG [89] from GERG-2008 EOS. For clarity the error bar for the combined expanded uncertainty (k = 2) in density measurement is plotted only for one measurement point.

EOS-CG is not shown in figure 4. The comparison of both EOS with the new experimental data looks similar.

For both (argon + carbon dioxide) mixtures, generally the experimental results agree with the GERG-2008 EOS within approximately 0.5%, which is within the uncertainty bounds of the GERG-2008 EOS stated for (argon + carbon dioxide) mixtures for the respective conditions. The deviations of the experimental data from the GERG-2008 EOS are much larger on (argon + carbon dioxide) mixtures than that on (nitrogen + carbon dioxide) mixtures, mainly because no binary specific departure function is available for the (argon + carbon dioxide) system in the GERG equation. The relative deviations between our experimental densities and the GERG EOS are strictly positive and increase with a higher amount of carbon dioxide in the mixture. For both binaries, deviations are temperature depended with the largest deviations at the lowest temperature (T = 298.15 K). All experimental data lie in a band of approximately 0.3% and show a similar consistent trend compared to the zero line (GERG-2008 EOS).

5. Conclusions

A single-sinker magnetic suspension densimeter was built to specifically investigate the (p,ρ,T,x) behavior of fluid mixtures relevant for CCS. To enable the investigation of supercritical states, also of corrosive substances, the densimeter was designed for measurements over the temperature range from (273.15 to 423.15) K with pressures up to 35 MPa. The expanded uncertainties (k = 2) were 35 mK for temperature, 3.39 kPa for pressure, and 0.033% for density. Within the scope of commissioning the new apparatus, measurements on pure nitrogen, argon, and carbon dioxide were carried out. For all three substances a similar pressure and temperature dependent systematic relative deviation compared to the respective EOS was observed. To compensate for this systematic deviation, a correction function only based on our current nitrogen measurements was applied. Although the correction function was only fitted to experimental densities for nitrogen, it worked well for all three pure substances. Later on, the correction function was applied for the data analysis of the mixture measurements.

The densimeter was used for measurements on the binary systems (nitrogen + carbon dioxide) and (argon + carbon dioxide). The compositions for both systems were (0.05 and 0.01) mole fraction carbon dioxide. Density measurements were carried out at temperatures from (298.15 to 423.15) K with pressures from (11 to 31) MPa. The relative combined expanded uncertainty (k = 2) in density was 0.15% for the (nitrogen + carbon dioxide) mixtures and 0.12% for the (argon + carbon dioxide) mixtures. A major contribution to this uncertainty emerged from the uncertainty in the composition of the gas mixtures. The new experimental data were compared to the GERG-2008 EOS and the EOS-CG. Relative deviations were within 0.1% for the (nitrogen + carbon dioxide) mixtures and mostly within 0.5% for the (argon + carbon dioxide) mixtures. The agreement of the new density values for the (0.95 nitrogen + 0.05 carbon dioxide) mixture with the only available literature data closest to the composition range under study, (0.90 nitrogen + 0.10 carbon dioxide) mixture of Mondéjar *et al.* [35], was better than 0.1%. The trend of both data sets was very consistent. This result suggests that the correction function, which we applied to our experimental densities for the gas mixtures, was an adequate means for our data analysis.

The experimental results of this work confirm the suitability of the GERG-2008 EOS and of the EOS-CG for the calculation of densities for the binary systems (nitrogen + carbon dioxide) and (argon + carbon dioxide) with carbon dioxide mole fractions up to 0.10 at temperatures from (298.15 to 423.15) K with pressures

from (11 to 31) MPa. The new experimental densities for the (argon + carbon dioxide) mixture could be used to further improve the performance of multi-parameter equations of state for mixtures.

Acknowledgements

The research leading to these results has received funding from the European Community's Seventh Framework Programme (*FP7-ENERGY-20121-1-2STAGE*) under Grant agreement No. 308809 (The IMPACTS Project). The authors acknowledge the project partners and the following funding partners for their contributions: Statoil Petroleum AS, Lundin Norway AS, Gas Natural Fenosa, MAN Diesel & Turbo SE and Vattenfall AB.

References

[1] R. Span, E.W. Lemmon, R.T. Jacobsen, W. Wagner, A. Yokozeki, J. Phys. Chem. Ref. Data 29 (2000) 1361–1433.
[2] C. Tegeler, R. Span, W. Wagner, J. Phys. Chem. Ref. Data 28 (1999) 779–850.
[3] R. Span, W. Wagner, J. Phys. Chem. Ref. Data 25 (1996) 1509–1596.
[4] D. Buecker, W. Wagner, J. Phys. Chem. Ref. Data 35 (2006) 205–266.
[5] J. Smukala, R. Span, W. Wagner, J. Phys. Chem. Ref. Data 29 (2000) 1053–1122.
[6] E.W. Lemmon, M.O. McLinden, W. Wagner, J. Chem. Eng. Data 54 (2009) 3141–3180.
[7] C. Guder, W. Wagner, J. Phys. Chem. Ref. Data 38 (2009) 33–94.
[8] M. Atilhan, S. Aparicio, S. Ejaz, D. Cristancho, K.R. Hall, J. Chem. Eng. Data 56 (2011) 212–221.
[9] M. Atilhan, S. Aparicio, S. Ejaz, D. Cristancho, I. Mantilla, K.R. Hall, J. Chem. Eng. Data 56 (2011) 3766–3774.
[10] M.E. Mondéjar, R.M. Villamañán, R. Span, C.R. Chamorro, J. Chem. Thermodyn. 48 (2012) 254–259.
[11] R. Hernández-Gómez, D. Tuma, M.A. Villamañán, M.E. Mondéjar, C.R. Chamorro, J. Chem. Thermodyn. 68 (2014) 253–259.
[12] O. Kunz, R. Klimeck, W. Wagner, M. Jaeschke, The GERG-2004 wide-range equation of state for natural gases and other mixtures. GERG Technical Monograph 15, Fortschr.-Ber. VDI, Reihe 6, Nr. 557, VDI-Verlag, Düsseldorf, 2007.
[13] O. Kunz, W. Wagner, J. Chem. Eng. Data 57 (2012) 3032–3091.
[14] E.W. Lemmon, R.T. Jacobsen, J. Phys. Chem. Ref. Data 33 (2004) 593–620.
[15] M. Atilhan, S. Ejaz, J. Zhou, D. Cristancho, I. Mantilla, J. Holste, K.R. Hall, J. Chem. Eng. Data 55 (2010) 4907–4911.
[16] E. De Visser, C. Hendriks, M. Barrio, M.J. Molnvik, G. De Koeijer, S. Liljemark, Y. Le Gallo, Int. J. Greenhouse Gas Control 2 (2008) 478–484.
[17] W. Wagner, K. Brachthäuser, R. Kleinrahm, H.W. Lösch, Int. J. Thermophys. 16 (1995) 399–411.
[18] K. Brachthäuser, R. Kleinrahm, H.W. Lösch, W. Wagner, Entwicklung eines neuen Dichtemeßverfahrens und Aufbau einer Hochtemperatur-Hochdruck-Dichtemeßanlage, Fortschr.-Ber. VDI, Reihe 8, Nr. 371, VDI-Verlag, Düsseldorf, 1993.
[19] R. Kleinrahm, W. Wagner, J. Chem. Thermodyn. 18 (1986) 739–760.
[20] W. Wagner, R. Kleinrahm, Metrologia 41 (2004) S24–S39.
[21] E. Wilhelm, T. Letcher, Volume Properties: Liquids, Solutions and Vapours, Royal Society of Chemistry, Cambridge, 2014.
[22] N. Kuramoto, K. Fujii, A. Waseda, Metrologia 41 (2004) S84–S94.
[23] M. Atilhan, High-accuracy, P–ρ–T Measurements up to 200 MPa Between 200 K to 500 K using a Single Sinker Magnetic Suspension Densitometer for Pure and Natural Gas like Mixtures (Dissertation), Texas A&M University, College Station, Texas, 2005.
[24] S. Ejaz, High-Accuracy P–ρ–T Measurements of Pure Gas and Natural Gas like Mixtures using a Compact Magnetic Suspension Densimeter (Dissertation), Texas A&M University, College Station, Texas, 2007.
[25] M.E. Mondéjar, J.J. Segovia, C.R. Chamorro, Measurement 44 (2011) 1768–1780.
[26] M. Richter, R. Kleinrahm, R. Span, P. Schley, GWF Int. 1 (2010) 66–69.
[27] M. Richter, R. Kleinrahm, R. Span, P. Schley, A new apparatus for accurate measurements of the densities of liquefied natural gas (LNG), International Gas Union Research Conference, Seoul, 2011.
[28] I.D. Mantilla, D.E. Cristancho, S. Ejaz, K.R. Hall, M. Atilhan, G.A. Iglesias-Silva, J. Chem. Eng. Data 55 (2010) 4227–4230.
[29] I.D. Mantilla, D.E. Cristancho, S. Ejaz, K.R. Hall, M. Atilhan, G.A. Iglesias-Silva, J. Chem. Eng. Data (2010) 1509–1596.
[30] D.E. Cristancho, I.D. Mantilla, S. Ejaz, K.R. Hall, M. Atilhan, G.A. Iglesias-Silva, J. Chem. Eng. Data (2010) 205–266.
[31] D.E. Cristancho, I.D. Mantilla, S. Ejaz, K.R. Hall, M. Atilhan, G.A. Iglesia-Silva, J. Chem. Eng. Data 55 (2009) 826–829.
[32] M. Atilhan, P.V. Patil, S. Ejaz, D. Cristancho, J. Holste, K.R. Hall, Wide range, high accuracy $P\rho T$ measurements by single sinker magnetic suspension densimeter for natural gas-like mixtures, in: H. Alfadala, G.V.R. Reklaitis, M.M. El-Halwagi (Eds.), Proceedings of the 1st Annual Gas Processing Symposium, Elsevier, Qatar, 2009.
[33] P. Patil, S. Ejaz, M. Atilhan, D. Cristancho, J.C. Holste, K.R. Hall, J. Chem. Thermodyn. 39 (2007) 1157–1163.
[34] C.R. Chamorro, J.J. Segovia, M.C. Martín, M.A. Villamañán, J.F. Estela-Uribe, J.P.M. Trusler, J. Chem. Thermodyn. 38 (2006) 916–922.
[35] M.E. Mondéjar, M.C. Martín, R. Span, C.R. Chamorro, J. Chem. Thermodyn. 43 (2011) 1950–1953.
[36] M.E. Mondéjar, T.E. Fernández-Vicente, F. Haloua, C.R. Chamorro, J. Chem. Eng. Data 57 (2012) 2581–2588.
[37] M.E. Mondéjar, M.A. Villamañán, R. Span, C.R. Chamorro, J. Chem. Eng. Data 56 (2011) 3933–3939.
[38] P. Claus, R. Kleinrahm, W. Wagner, J. Chem. Thermodyn. 35 (2003) 159–175.
[39] D. Sommer, R. Kleinrahm, R. Span, W. Wagner, J. Chem. Thermodyn. 43 (2011) 117–132.
[40] G. Schilling, R. Kleinrahm, W. Wagner, J. Chem. Thermodyn. 40 (2008) 1095–1105.
[41] J. Klimeck, R. Kleinrahm, W. Wagner, J. Chem. Thermodyn. 30 (1998) 1571–1588.
[42] J. Klimeck, R. Kleinrahm, J. Chem. Thermodyn. 33 (2001) 251–267.
[43] R. Wegge, M. Richter, R. Span, Personal Communication, Lehrstuhl für Thermodynamik, Ruhr-Universität Bochum, Germany, 2015.
[44] B. Metz, O. Davidson, H. De Coninck, M. Loos, L. Meyer, Carbon Dioxide Capture and Storage, IPCC Geneva, Switzerland, 2005.
[45] G. Pipitone, O. Bolland, Int. J. Greenhouse Gas Control 3 (2009) 528–534.
[46] W.H. Abraham, C.O. Bennett, AIChE J. 6 (1960) 257–261.
[47] E. Sarashina, Y. Arai, S. Sasto, J. Chem. Eng. Jpn. 4 (1971) 379–381.
[48] W. Schönmann, Messung der thermischen Eigenschaften und Aufstellung einer empirischen Zustandsgleichung gasförmiger Argon-Kohlendioxid-Gemische, Dissertation, Fakultät für Chemieingenieurwesen, Universität Karlsruhe, Karlsruhe, 1971.
[49] N.D. Kosov, I.S. Brovanov, Teploenergetika 22 (1975) 87–89.
[50] V.V. Altunin, O.D. Koposhilov, Trudy Moskovskogo Energeticheskogo Instituta 313 (1976) 20–23.
[51] V.V. Altunin, O.D. Koposhilov, Teploenergetika 24 (1977) 66–70.
[52] M. Mantovani, P. Chiesa, G. Valenti, M. Gatti, S. Consonni, J. Supercrit. Fluids 61 (2012) 34–43.
[53] I.R. Kritschewsky, V.P. Markov, Acta Physicochim. URS 12 (1940) 59–66.
[54] A.E. Edwards, W.E. Roseveare, JACS 64 (1942) 2816–2819.
[55] R.E.D. Haney, H. Bliss, Ind. Eng. Chem. 36 (1944) 985–989.
[56] R.A. Gorski, J.G. Miller, JACS 75 (1953) 550–552.
[57] Y. Arai, G.I. Kaminishi, S. Saito, J. Chem. Eng. Jpn. 4 (1971) 113–122.
[58] V.V. Altunin, D.H. Chin, Trudy Moskovskogo Energeticheskogo Instituta 111 (1972) 64–70.
[59] S.L. Rivkin, Thermophys. Prop. Matter Substances 8 (1975) 190–209.
[60] G. Kaminishi, Koatsu Gasu 15 (1978) 177–183.
[61] J.F. Ely, W.M. Haynes, J.W. Magee, Research Report RR-110, Thermophysical Properties for Special High CO2 Content Mixtures, Gas Processors Association, Tulsa, 1987.
[62] A. Hacura, J.H. Yoon, F.G. Baglin, J. Chem. Eng. Data 33 (1988) 152–154.
[63] H.B. Brugge, C.-A. Hwang, W.J. Rogers, J.C. Holste, K.R. Hall, W. Lemming, G.J. Esper, K.N. Marsh, B.E. Gammon, Physica A 156 (1989) 382–416.
[64] P. McElroy, R. Battino, M. Dowd, J. Chem. Thermodyn. 21 (1989) 1287–1300.
[65] G.J. Esper, D.M. Bailey, J.C. Holste, K.R. Hall, Fluid Phase Equilib. 49 (1989) 35–47.
[66] J.F. Ely, W.M. Haynes, B.C. Bain, J. Chem. Thermodyn. 21 (1989) 879–894.
[67] D.M. Bailey, G.J. Esper, J.C. Holste, K.R. Hall, P.T. Eubank, K.N. Marsh, W.J. Rogers, Research Report RR-122, Properties of CO2 Mixtures with N2 and with CH4, Gas Processors Association, Tulsa, 1989.
[68] S. Jiang, Y. Wang, J. Shi, Fluid Phase Equilib. 57 (1990) 105–117.
[69] M. Jaeschke, A.E. Humphreys, The GERG databank of high accuracy compressibility factor measurements, GERG Technical Monograph 4, Fortschr.-Ber. VDI, Reihe 6, Nr. 251, VDI-Verlag, Düsseldorf, 1991.
[70] J.C. Seitz, J.G. Blencoe, D.B. Joyce, R.J. Bodnar, Geochim. Cosmochim. Acta 58 (1994) 1065–1071.
[71] H.A. Duarte-Garza, J.C. Holste, K.R. Hall, K.N. Marsh, B.E. Gammon, J. Chem. Eng. Data 40 (1995) 704–711.
[72] H. Duarte-Garza, H.B. Brugge, C.-A. Hwang, P.T. Eubank, J.C. Holste, K.R. Hall, B.E. Gammon, K.N. Marsh, Research Report RR-140, Thermodynamic Properties of CO2 + N2 Mixtures, Gas Processors Association/Gas Research Institute, 1995.
[73] J.C. Seitz, J.G. Blencoe, J. Chem. Thermodyn. 28 (1996) 1207–1213.
[74] J.C. Seitz, J.G. Blencoe, R.J. Bodnar, J. Chem. Thermodyn. 28 (1996) 521–538.
[75] H.B. Brugge, J.C. Holste, K.R. Hall, B.E. Gammon, K.N. Marsh, J. Chem. Eng. Data 42 (1997) 903–907.
[76] JCGM, Evaluation of measurement data – guide to the expression of uncertainty in measurement, BIPM, Sèvres, 2008.
[77] H. Watanabe, N. Yamada, M. Okaji, Int. J. Thermophys. 25 (2004) 221–236.
[78] J.J. Hall, Phys. Rev. 161 (1967) 756.
[79] Landolt-Börnstein, Elastic Constants of Second Order: Temperature Coefficients Tc, Springer Verlag, Berlin, 2001.
[80] M. Richter, R. Kleinrahm, J. Chem. Thermodyn. 74 (2014) 58–66.
[81] M.O. McLinden, R. Kleinrahm, W. Wagner, Int. J. Thermophys. 28 (2007) 429–448.
[82] D.E. Cristancho, I.D. Mantilla, S. Ejaz, K.R. Hall, G.A. Iglesias-Silva, M. Atilhan, Int. J. Thermophys. 31 (2010) 698–709.
[83] Y. Kayukawa, Y. Kano, K. Fujii, H. Sato, Metrologia 49 (2012) 513–521.
[84] Y. Kano, Y. Kayukawa, K. Fujii, H. Sato, Meas. Sci. Technol. 18 (2007) 659–666.

[85] J. Klimeck, Weiterentwicklung einer Ein-Senkkörper Dichtemessanlage und Präzisionsmessungen der thermischen Zustandsgrößen von Kohlendioxid, Argon, Stickstoff und Methan, Dissertation, Ruhr-University Bochum, Bochum, 1997.
[86] E.W. Lemmon, M.L. Huber, M.O. McLinden, NIST Standard Reference Database 23: Reference Fluid Thermodynamic and Transport Properties-REFPROP, Version 9.1, National Institute of Standards and Technology, Boulder, 2013.
[87] J. Gernert, A New Helmholtz Energy Model for Humid Gases and CCS Mixtures (Dissertation), Ruhr University Bochum, Bochum, 2013.
[88] J. Gernert, R. Span, J. Chem. Thermodyn. (2015), http://dx.doi.org/10.1016/j.jct.2015.05.015.
[89] R. Span, T. Eckermann, J. Gernert, S. Herrig, A. Jäger, M. Thol, TREND. Thermodynamic Reference and Engineering Data 1.1, Lehrstuhl für Thermodynamik, Ruhr-Universitaet Bochum, 2014.

JCT 15-263